Available online at www.sciencedirect.com
SCIENCE DIRECT®
Journal of Computational Physics 199 (2004) 87–109
JOURNAL OF COMPUTATIONAL PHYSICS
www.elsevier.com/locate/jcp

WENO schemes for balance laws with spatially varying flux ☆

Senka Vukovic *, Nelida Crnjaric-Zic, Luka Sopta

Faculty of Engineering, University of Rijeka, 51000 Rijeka, Vukovarska 58, Croatia

Received 26 May 2003; received in revised form 3 February 2004; accepted 3 February 2004
Available online 5 March 2004

Abstract

In this paper we construct numerical schemes of high order of accuracy for hyperbolic balance law systems with spatially variable flux function and a source term of the geometrical type. We start with the original finite difference characteristicwise weighted essentially nonoscillatory (WENO) schemes and then we create new schemes by modifying the flux formulations (locally Lax-Friedrichs and Roe with entropy fix) in order to account for the spatially variable flux, and by decomposing the source term in order to obtain balance between numerical approximations of the flux gradient and of the source term. We apply so extended WENO schemes to the one-dimensional open channel flow equations and to the one-dimensional elastic wave equations. In particular, we prove that in these applications the new schemes are exactly consistent with steady-state solutions from an appropriately chosen subset. Experimentally obtained orders of accuracy of the extended and original WENO schemes are almost identical on a convergence test. Other presented test problems illustrate the improvement of the proposed schemes relative to the original WENO schemes combined with the pointwise source term evaluation. As expected, the increase in the formal order of accuracy of applied WENO reconstructions in all the tests causes visible increase in the high resolution properties of the schemes.

PACS: 65M06; 76M20; 25L65

Keywords: Hyperbolic balance laws; Spatially varying flux; Flux gradient and source term balancing; Open channel flow equations; Elastic wave equations

1. Introduction

In this paper, we propose numerical schemes of high order of accuracy particularly designed for balance law systems with spatially varying flux and geometrical source term. Two such balance law systems of particular interest in applications are open channel flow equations and elastic wave equations.

☆ This work was supported by the Ministry of Science and Technology of Republic of Croatia.
* Corresponding author. Tel.: +385-51-651-497; fax: +385-51-651-490.
E-mail addresses: senka.vukovic@ri.hinet.hr (S. Vukovic), nelida@riteh.hr (N. Crnjaric-Zic), luka.sopta@riteh.hr (L. Sopta).

0021-9991/$ - see front matter
doi:10.1016/j.jcp.2004.02.002

The way how to treat difficulties that arise from geometrical source terms is by now well known and consist in creating a well-balanced scheme [12,13], possibly with exact conservation property [3,4]. There are numerous results in this area that begin with the work of Bermùdez and Vázquez [4], and then papers of Greenberg and LeRoux [11], Bermùdez et al. [3], LeVeque [21], Jenny and Müller [18], Bristeau and Perthame [5], Chinnaya and LeRoux [7], Gosse [12,13], Hubbard and García–Navarro [17], Jin [20], Perthame and Simeoni [23], Zhou et al. [31], etc. follow. Most of these results are concerned with shallow water equations, and some with transport of a pollutant or temperature in shallow waters, or with chemical Euler equations.

On the other hand, when we add a spatially variable flux, there are fewer known results. In particular, Vázquez [28], Hubbard and García-Navarro [17], García-Navarro and Vázquez-Cendón [10], and Burguete and García-Navarro [6] treat this problem for the case of open channel flow equations. However, typically the case of rectangular cross-section channel geometry is discussed, and much more rarely the general case of completely irregular channel geometry is taken into consideration. In particular, in [30] we solved this general case with appropriately modified upwind schemes – Q-scheme and flux limited scheme. Furthermore, Bale et al. [1] deal with the balance laws with spatially variable flux functions, give a new version of the wave propagation method and apply it to elastic wave equations.

We must emphasize that in all the known results proposed schemes for balance laws of the discussed type are at most of the second order of accuracy. Therefore, there is a need for well-balanced schemes with higher orders of accuracy. A very well-known set of high order and shock capturing schemes are the essentially nonoscillatory (ENO) and the weighted essentially nonoscillatory (WENO) schemes. ENO schemes were developed by Harten and Osher [15,16], and WENO were first proposed by Liu et al. [22]. These schemes were originally designed for hyperbolic conservation laws with autonomous, i.e., not spatially variable, flux functions. In [29] we extended the finite difference version of these schemes to new schemes for hyperbolic balance laws with geometrical source term and applied them successfully to shallow water equations, i.e., we obtained schemes that are well balanced, and even more exactly consistent with quiescent flow. We proposed a similar WENO extension for the sediment transport equations in [8]. The work we present now is a direct continuation of these papers.

In fact, here, we create a new algorithm, which is a natural extension of the original schemes as well as the ones we presented before. In particular, we present extensions for finite difference versions of locally Lax-Friedrichs and Roe with entropy fix formulations. In Sections 2 and 3 we extend the original schemes to one-dimensional open channel flow equations and to one-dimensional elastic wave equations, respectively. Section 4 contains the generalization of the new algorithms, as well the conditions on the terms in the general algorithm that guarantee the schemes are consistent with any chosen subset of steady-state solutions. Finally, in Section 5 we present a convergence test and several test problems aimed on testing the improvement of the schemes when compared with the original WENO schemes combined with pointwise source term evaluation, and also aimed on testing high resolution properties of the schemes.

2. Extension of WENO schemes to one-dimensional open channel flow equations

The one-dimensional open channel flow equations [9] consist of the mass conservation law and the momentum balance law

$$\begin{aligned} &\frac{\partial A}{\partial t}+\frac{\partial Q}{\partial x}=0,\\ &\frac{\partial Q}{\partial t}+\frac{\partial}{\partial x}\left(\frac{Q^2}{A}+gI_1\right)=g\left(I_2-A\frac{\mathrm{d}z}{\mathrm{d}x}\right). \end{aligned} \tag{1}$$

Here, t is the time, x is the space coordinate, $A = A(x,t)$ is the wetted cross-section area, $Q = Q(x,t)$ is the discharge, g is the acceleration due to gravity, and $z = z(x)$ is the bed level. In particular, discharge and water velocity $v = v(x,t)$ are related as $Q = A \cdot v$. Furthermore, $I_1 = I_1(x,h) = \int_0^h (h-\zeta)B(x,\zeta)\mathrm{d}\zeta$ is the hydrostatic pressure force term. Here, $h = h(x,A)$ is the water depth and $B = B(x,\zeta)$ is the channel width. Obviously they are connected through relation $A = \int_0^h B(x,\zeta)\mathrm{d}\zeta$. Finally, $I_2 = I_2(x,h) = \int_0^h (h-\zeta)\frac{\partial B}{\partial x}(x,\zeta)\mathrm{d}\zeta$ is the term that accounts for the forces exerted by the channel walls at contractions and expansions. Open channel flow equations also have an additional source term that models friction forces. It is the term $-gA(M^2Q|Q|/A^{2/3}P^{4/3})$ that must be added to the right-hand side of the second equation in (1). In that friction term, $M = M(x)$ is the Manning friction factor and $P = P(x,A)$ is the wetted area perimeter.

In fact, system of balance laws (1) is of type

$$\partial_t \mathbf{u} + \partial_x \mathbf{f}(\mathbf{u},x) = \mathbf{g}(\mathbf{u},x) \tag{2}$$

with

$$\mathbf{u} = \begin{pmatrix} A \\ Q \end{pmatrix}, \quad \mathbf{f} = \begin{pmatrix} Q \\ \frac{Q^2}{A} + gI_1 \end{pmatrix}, \quad \mathbf{g} = \begin{pmatrix} 0 \\ gI_2 - gA\frac{\mathrm{d}z}{\mathrm{d}x} \end{pmatrix}. \tag{3}$$

Here, $\mathbf{u}$ is the vector of conserved variables, $\mathbf{f}$ is the flux, and $\mathbf{g}$ is the source term.

Our goal is to numerically solve (1) by application of finite difference WENO schemes. We immediately see that we must face two difficulties that are not covered with the original WENO algorithms: the flux is spatially variable and the source term is of the geometrical type. Therefore, we need to extend the original WENO schemes, and we proceed as follows.

Typically in finite difference WENO schemes numerical computations are divided in two separate tasks. The first task is the integration in time for the system in consideration. For that purpose the system is rewritten in the form $\partial_t \mathbf{u} = \mathbf{L}$ with $\mathbf{L} = -\partial_x \mathbf{f} + \mathbf{g}$, and this task is solved by a Runge–Kutta type method [27]. Since the difficulties that arise in the case (2) are related to the space coordinate, it is clear that there is no need for our intervention in this part of the algorithm.

The second task is the numerical approximation of $\mathbf{L}$. More precisely, if a space discretization with cells $[x_{i-1/2}, x_{i+1/2}]$ of uniform width Δx is assumed and if a numerical approximation $\mathbf{u}_i$, $i = 1,\ldots,N$ to the solution $\mathbf{u}$ in the ith cell center at any time t is known, an algorithm for the evaluation of $\mathbf{L}_i$, $i = 1,\ldots,N$ in the form

$$\mathbf{L}_i = \frac{-1}{\Delta x}(\mathbf{f}_{i+1/2} - \mathbf{f}_{i-1/2}) + \mathbf{g}_i \tag{4}$$

must be proposed. Here $\mathbf{f}_{i+1/2}$, $i = 0,\ldots,N$ is the numerical flux at the $(i+1/2)$th cell boundary and $\mathbf{g}_i$, $i = 1,\ldots,N$ is the numerical source term in the ith cell.

In many cases when the source term is present a simple pointwise evaluation, i.e., $\mathbf{g}_i = \mathbf{g}(\mathbf{u}_i, x_i)$ works well. In particular, this approach is good enough for the friction term as we discussed in [29,30]. However, this approach gives very poor results if the source term is of the geometrical type. In fact, as it is proposed in [4] a decomposition of the geometrical source term of the form

$$\mathbf{g}_i = \mathbf{g}_{i-1/2,R} + \mathbf{g}_{i+1/2,L} \tag{5}$$

is necessary. This decomposition of the source term takes into account the need to include upwinding in the source term approximations, which improves the stability of the scheme, as it was shown by Roe in [24]. In addition it is consistent with the conservation scheme approach to evaluation of the flux gradient (4) and therefore helps in achieving the balance between the numerical approximations of the flux gradient and of the source term. Therefore, in the case (2) we must use relation (5).

Thus, we are left with the problem of constructing appropriate expressions for numerical approximations $\mathbf{f}_{i+1/2}$, $\mathbf{g}_{i+1/2,L}$, and $\mathbf{g}_{i+1/2,R}$, $i = 0, \ldots, N$. At this point we must make a choice between coordinatewise and characteristicwise approach and we choose the second one. Therefore, we need to compute an approximation of the local characteristic fields for each $(i+1/2)$th cell boundary, i.e., we need some numerical approximation $\mathbf{A}_{i+1/2}$ to the Jacobian matrix of the flux $\mathbf{A} = \frac{\partial \mathbf{f}}{\partial \mathbf{u}}$ at the $(i+1/2)$th cell boundary. Since in the case (2) the flux is explicitly dependent on the space coordinate we must at the same time take in consideration an additional term $\mathbf{v} = \frac{\partial \mathbf{f}}{\partial x}$ [17], and bear in mind that $\mathrm{d}\mathbf{f} = \mathbf{A}\,\mathrm{d}\mathbf{u} + \mathbf{v}\,\mathrm{d}x$. Therefore, we propose to use a natural extension for the standard Roe average relation [30]

$$\mathbf{f}_{i+1} - \mathbf{f}_i = \mathbf{A}\big(\mathbf{u}_{i+1/2,\mathrm{ERoe}}, x_{i+1/2}\big)\big(\mathbf{u}_{i+1} - \mathbf{u}_i\big) + \mathbf{v}_{i+1/2} \cdot \Delta x \tag{6}$$

for the definition of the extended Roe average $\mathbf{u}_{i+1/2,\mathrm{ERoe}}$. Here we must emphasize that we do not assume $\mathbf{v}_{i+1/2} = \mathbf{v}(\mathbf{u}_{i+1/2,\mathrm{ERoe}}, x_{i+1/2})$, since that would be too restrictive for Eq. (6). Instead, we assume a more general form

$$\mathbf{v}_{i+1/2} = \frac{1}{\Delta x}\mathscr{V}(\mathbf{u}_i, \mathbf{u}_{i+1}, x_i, x_{i+1}), \tag{7}$$

where the expression for $\mathscr{V} = \mathscr{V}(\mathbf{u}', \mathbf{u}'', x', x'')$ is obtained as a numerical approximation for $\mathbf{v}\,\mathrm{d}x$.

In particular, in our case of open channel flow equations (1) we compute [30]

$$\mathbf{A} = \begin{pmatrix} 0 & 1 \\ c^2 - v^2 & 2v \end{pmatrix} \quad \text{and} \quad \mathbf{v} = \begin{pmatrix} 0 \\ g\big(I_2 - \frac{A}{B}D\big) \end{pmatrix}, \tag{8}$$

where we introduce $D = \frac{\partial A}{\partial x}\big|_{h=\mathrm{const.}}$ and $c = \sqrt{g(A/B)}$. If we just put the subscript $(i+1/2)$ on the terms in (8) we will not be able to solve Eq. (6). Therefore, we reformulate the expression for $\mathbf{v}\,\mathrm{d}x$ and obtain [30]

$$\mathbf{v}\,\mathrm{d}x = \begin{pmatrix} 0 \\ g\,\mathrm{d}I_1 - g\frac{A}{B}\mathrm{d}A \end{pmatrix}. \tag{9}$$

Now a natural numerical approximation for $\mathbf{v}\,\mathrm{d}x$ appears to us

$$\mathscr{V} = \begin{pmatrix} 0 \\ g\big(I_1'' - I_1'\big) - g\frac{A'+A''}{B'+B''}\big(A'' - A'\big) \end{pmatrix}. \tag{10}$$

If we use this, we immediately see that the equation in the first coordinate of (6) is trivially satisfied, while the equation in the second coordinate transforms into

$$\begin{aligned}\left(\frac{Q_{i+1}^2}{A_{i+1}} - \frac{Q_i^2}{A_i}\right) + g(I_{1,i+1} - I_{1,i}) &= c_{i+1/2}^2(A_{i+1} - A_i) - v_{i+1/2}^2(A_{i+1} - A_i) + 2v_{i+1/2}(Q_{i+1} - Q_i) \\ &\quad + g(I_{1,i+1} - I_{1,i}) - g\frac{A_i + A_{i+1}}{B_i + B_{i+1}}(A_{i+1} - A_i).\end{aligned} \tag{11}$$

Here the second term on the left-hand side and the fourth term on the right-hand side are equal. Additionally, if we use approximation

$$c_{i+1/2} = \sqrt{g\frac{A_i + A_{i+1}}{B_i + B_{i+1}}} \tag{12}$$

also the first and the last term on the right-hand side of (11) become equal. For the remaining terms in (11) standard computations used in Roe average evaluation lead us to

$$v_{i+1/2} = \frac{\sqrt{A_i}v_i + \sqrt{A_{i+1}}v_{i+1}}{\sqrt{A_i} + \sqrt{A_{i+1}}}. \tag{13}$$

Thus, we found the extended Roe average.

Now local characteristic fields, i.e., eigenvalues $\lambda^{(p)}_{i+1/2}$, right eigenvectors $\mathbf{r}^{(p)}_{i+1/2}$, and left eigenvectors $\mathbf{l}^{(p)}_{i+1/2}$, $p = 1, \ldots, m$, at the $(i + 1/2)$th cell boundary can be computed. Here, m is the number of equations in the hyperbolic system of balance laws (2). In our case of open channel flow equations $m = 2$, while eigenvalues, left, and right eigenvectors are $\lambda^{(p)} = v + (-1)^p c,\ p = 1, 2,$

$$\mathbf{r}^{(p)} = \begin{pmatrix} 1 \\ \lambda^{(p)} \end{pmatrix},\ \mathbf{l}^{(p)} = \frac{1}{2c}\begin{pmatrix} (-1)^{q(p)}\lambda^{q(p)} \\ (-1)^p \end{pmatrix}, \quad p = 1, 2, \tag{14}$$

where $q(1) = 2$ and $q(2) = 1$. Then, we can proceed with the construction of characteristicwise components $f^{(p)}_{i+1/2}$, $g^{(p)}_{i+1/2,L}$, and $g^{(p)}_{i+1/2,R}$, $p = 1, \ldots, m$, $i = 0, \ldots, N$.

Before we continue the construction we must remind ourselves that the goal is to achieve a numerical scheme that is balanced. In particular, in the case of steady-state solutions the flux gradient and the source term cancel out in the hyperbolic balance laws, i.e., these two terms are in balance. Therefore, a scheme will be consistent with that property if it exactly conserves any steady-state solution, i.e., if

$$\mathbf{L}_i = \mathbf{0}, \quad i = 1, \ldots, N, \tag{15}$$

is true for all steady states. However, such a condition is usually too complicated to achieve for all steady-state solutions, so consistency of the scheme is usually requested only for some particular subset of steady-state solutions. For example, in the case of open channel flow equations (1) we demand from a scheme to be consistent with the quiescent flow

$$H = \text{const.} \quad \text{and} \quad v = 0. \tag{16}$$

In general, when such consistency is present we say that the scheme has the exact conservation property [3] for the referent subset of steady-state solutions.

2.1. The local Lax-Friedrichs formulation

Let us now concentrate on the local Lax-Friedrichs (LLF) formulation. Since our goal is to create a balanced scheme, we compare the original LLF algorithm with the balanced Q-scheme [4], and we propose numerical approximation of the flux in the form

$$f^{(p)}_{i+1/2} = f^{(p)}_{i+1/2,\text{Q-scheme}} + \mathscr{P}^{(p)}_{i+1/2,+} + \mathscr{P}^{(p)}_{i+1/2,-}, \tag{17}$$

and numerical approximation for the source term in the form

$$g^{(p)}_{i+1/2,L} = g^{(p)}_{i+1/2,L,\text{Q-scheme}} + \frac{1}{\Delta x}\mathscr{Q}^{(p)}_{i+1/2,+} + \frac{1}{\Delta x}\mathscr{Q}^{(p)}_{i+1/2,-}, \tag{18}$$

$$g^{(p)}_{i+1/2,R} = g^{(p)}_{i+1/2,R,\text{Q-scheme}} - \frac{1}{\Delta x}\mathscr{Q}^{(p)}_{i+1/2,+} - \frac{1}{\Delta x}\mathscr{Q}^{(p)}_{i+1/2,-}. \tag{19}$$

The separation of the Q-scheme parts from the high-order WENO reconstruction terms $\mathscr{P}^{(p)}_{i+1/2,\pm}$ and $\mathscr{Q}^{(p)}_{i+1/2,\pm}$ was one of the key ideas that we introduced in [29] and it is reasonable to suppose that it is a good starting point now too. Before we proceed, let us see what is the effect of this approach on the desired exact conservation property. If we insert (17)–(19) into (4) and rearrange, for the pth characteristicwise component we obtain

$$L_i^p = L_{i,\text{Q-scheme}}^p - \frac{1}{\Delta x}\left(\mathscr{P}_{i+1/2,+}^{(p)} - \mathscr{Q}_{i+1/2,+}^{(p)}\right) - \frac{1}{\Delta x}\left(\mathscr{P}_{i+1/2,-}^{(p)} - \mathscr{Q}_{i+1/2,-}^{(p)}\right) + \frac{1}{\Delta x}\left(\mathscr{P}_{i-1/2,+}^{(p)} - \mathscr{Q}_{i-1/2,+}^{(p)}\right) + \frac{1}{\Delta x}\left(\mathscr{P}_{i-1/2,-}^{(p)} - \mathscr{Q}_{i-1/2,-}^{(p)}\right). \tag{20}$$

Here

$$L_{i,\text{Q-scheme}}^p = -\frac{1}{\Delta x}\left(f_{i+1/2,\text{Q-scheme}}^{(p)} - f_{i-1/2,\text{Q-scheme}}^{(p)}\right) + g_{i-1/2,R,\text{Q-scheme}}^{(p)} + g_{i+1/2,L,\text{Q-scheme}}^{(p)} \tag{21}$$

is the Q-scheme part, i.e., it consists of the Q-scheme variant for the spatially variable flux

$$f_{i+1/2,\text{Q-scheme}}^{(p)} = \frac{1}{2}\left((\mathbf{f}_i + \mathbf{f}_{i+1}) - \left|\lambda_{i+1/2}^{(p)}\right|(\mathbf{u}_{i+1} - \mathbf{u}_i) - \operatorname{sign}\left(\lambda_{i+1/2}^{(p)}\right)\mathbf{v}_{i+1/2}\Delta x\right) \cdot \mathbf{l}_{i+1/2}^{(p)} \tag{22}$$

and of the Q-scheme geometrical source term expressions

$$g_{i+1/2,L,\text{Q-scheme}}^{(p)} = \frac{1 - \operatorname{sign}\left(\lambda_{i+1/2}^{(p)}\right)}{2}\mathbf{g}_{i+1/2} \cdot \mathbf{l}_{i+1/2}^{(p)}, \tag{23}$$

$$g_{i+1/2,R,\text{Q-scheme}}^{(p)} = \frac{1 + \operatorname{sign}\left(\lambda_{i+1/2}^{(p)}\right)}{2}\mathbf{g}_{i+1/2} \cdot \mathbf{l}_{i+1/2}^{(p)}. \tag{24}$$

In (22) $\mathbf{v}_{i+1/2}$ is given with (7), while in (23) and (24) $\mathbf{g}_{i+1/2}$ is given with

$$\mathbf{g}_{i+1/2} = \frac{1}{\Delta x}\mathscr{G}(\mathbf{u}_i, \mathbf{u}_{i+1}, x_i, x_{i+1}), \tag{25}$$

where $\mathscr{G} = \mathscr{G}(\mathbf{u}', \mathbf{u}'', x', x'')$ is the numerical approximation for $\mathbf{g}\Delta x$. In particular, in the open channel flow equations (1) case we compute [30]

$$\mathbf{g}\,\mathrm{d}x = \begin{pmatrix} 0 \\ g\,\mathrm{d}I_1 - gA\,\mathrm{d}H \end{pmatrix}. \tag{26}$$

Here, $H = h + z$ is the water level. Therefore, a natural choice becomes obvious to us

$$\mathscr{G} = \begin{pmatrix} 0 \\ g(I_1'' - I_1') - g\frac{A'+A''}{2}(H'' - H') \end{pmatrix}. \tag{27}$$

For open channel equations the complete construction of the Q-scheme that guarantees its exact conservation property is known [30]. Since (21) is the part of (20) that we do not have to examine further, we can concentrate only on the WENO reconstruction terms. In fact, if we can obtain that for the chosen subset of steady-state solutions

$$\mathscr{P}_{i+1/2,\pm}^{(p)} - \mathscr{Q}_{i+1/2,\pm}^{(p)} = 0 \tag{28}$$

is true, then (20) will vanish and the exact conservation property will be obtained. Furthermore, $\mathscr{P}_{i+1/2,\pm}^{(p)}$ and $\mathscr{Q}_{i+1/2,\pm}^{(p)}$ are WENO reconstructions terms for some appropriately chosen functions $v^{\pm}$, related to $\mathbf{f}$, and $w^{\pm}$, related to $\mathbf{g}\,\mathrm{d}x$, respectively. Therefore, they are computed as

$$\mathscr{P}_{i+1/2,\pm}^{(p)} = \sum_{s=s_{\min}^{\pm}}^{s_{\max}^{\pm}} \sum_{j=0}^{r} \omega_{r,s} a_{r,s,j}^{\pm} v_{i-r+s+j}^{\pm}, \tag{29}$$

$$\mathscr{Q}^{(p)}_{i+1/2,\pm} = \sum_{s=s^{\pm}_{\min}}^{s^{\pm}_{\max}} \sum_{j=0}^{r} \omega_{r,s} a^{\pm}_{r,s,j} w^{\pm}_{i-r+s+j}. \tag{30}$$

Here, $s^{+}_{\min} = 0$, $s^{+}_{\max} = r$, $s^{-}_{\min} = 1$, and $s^{-}_{\max} = r+1$ define the first and the last stencil of points $S^{\pm}_{r,s} = \{x_{i-r+s}, \ldots, x_{i+s}\}$, $s = s^{\pm}_{\min}, \ldots, s^{\pm}_{\max}$ to be used; $\omega_{r,s}$, $s = s^{\pm}_{\min}, \ldots, s^{\pm}_{\max}$ are the weight values associated with the $S^{\pm}_{r,s}$ stencil; $a^{\pm}_{r,s,j}$, $s = s^{\pm}_{\min}, \ldots, s^{\pm}_{\max}$, $j = 0, \ldots, r$ are some precomputed interpolation coefficients; and $v^{\pm}_k = v^{\pm}(x_k)$, $w^{\pm}_k = w^{\pm}(x_k)$, $k = 0, \ldots, N$. The weights $\omega_{r,s}$, $s = s^{\pm}_{\min}, \ldots, s^{\pm}_{\max}$ are derived as usually in the WENO reconstruction algorithms from smoothness measures along each stencil. In the typical approach the weights for $\mathscr{P}^{(p)}_{i+1/2,\pm}$ would be computed from smoothness measures for functions $v^{\pm}$, and the weights for $\mathscr{Q}^{(p)}_{i+1/2,\pm}$ from smoothness measures for functions $w^{\pm}$. However, in the expression for (20) only differences $\mathscr{P}^{(p)}_{i+1/2,\pm} - \mathscr{Q}^{(p)}_{i+1/2,\pm}$ appear, so we decide to use the same weights for both reconstructions, weights computed from smoothness measures for functions $v^{\pm} - w^{\pm}$. Then using (29) and (30) we obtain

$$\mathscr{P}^{(p)}_{i+1/2,\pm} - \mathscr{Q}^{(p)}_{i+1/2,\pm} = \sum_{s=s^{\pm}_{\min}}^{s^{\pm}_{\max}} \sum_{j=0}^{r} \omega_{r,s} a^{\pm}_{r,s,j} \left(v^{\pm}_{i-r+s+j} - w^{\pm}_{i-r+s+j} \right), \tag{31}$$

so this idea becomes crucial for the correct balancing results. In fact, now from (31) an obvious conclusion appears – if we can define $v^{\pm}$ and $w^{\pm}$ in such a way that they are not only meaningful numerical approximations for $\mathbf{f}$ and $\mathbf{g}\,\mathrm{d}x$, respectively, but also such that

$$v^{\pm} - w^{\pm} = 0 \tag{32}$$

is true for some subset of steady-state solutions, our goal will be achieved.

Therefore, let us first deal with $v^{\pm}$ functions. In [30] we showed that if for the case of hyperbolic conservation laws with autonomous flux we use

$$v^{\pm} = \frac{1}{2} \left(\left(\mathbf{f} \pm \left| \lambda^{(p)}_{i+1/2} \right| \mathbf{u} \right) - \left(\mathbf{f}_{I^{\pm}} \pm \left| \lambda^{(p)}_{i+1/2} \right| \mathbf{u}_{I^{\pm}} \right) \right) \cdot \mathbf{l}^{(p)}_{i+1/2}, \tag{33}$$

with $I^{+} = i$ and $I^{-} = i+1$, then the proposed algorithm is identical to the original LLF formulation. However, now we have a spatially variable flux function, so the standard LLF formulation is not acceptable. In fact, in order to compensate for the $\mathbf{v}_{i+1/2}\Delta x$ term in (22) we could use

$$v^{\pm} = \frac{1}{2} \left((\mathbf{f} - \mathbf{f}_{I^{\pm}}) \pm \left| \lambda^{(p)}_{i+1/2} \right| (\mathbf{u} - \mathbf{u}_{I^{\pm}}) \pm \operatorname{sign}\left(\lambda^{(p)}_{i+1/2} \right) \mathscr{V}(\mathbf{u}_{I^{\pm}}, \mathbf{u}, x_{I^{\pm}}, x) \right) \cdot \mathbf{l}^{(p)}_{i+1/2}. \tag{34}$$

Furthermore, for $w^{\pm}$ a possible first idea is to use

$$w^{\pm} = \frac{1 \pm \operatorname{sign}\left(\lambda^{(p)}_{i+1/2} \right)}{2} \mathscr{G}(\mathbf{u}_{I^{\pm}}, \mathbf{u}, x_{I^{\pm}}, x) \cdot \mathbf{l}^{(p)}_{i+1/2}. \tag{35}$$

These two choices seem like acceptable numerical approximations. In particular, for open channel flow equations (1) under the quiescent flow conditions (16) we get

$$v^{\pm} = \frac{1}{2c_{i+1/2}} \left(g \left(\frac{A_i + A_{i+1}}{B_i + B_{i+1}} - \frac{A + A_{I^{\pm}}}{B + B_{I^{\pm}}} \right) (A - A_{I^{\pm}}) + ((-1)^p \pm 1) g (I_1 - I_{1,I^{\pm}}) \right), \tag{36}$$

$$w^{\pm} = \frac{1}{2c_{i+1/2}} ((-1)^p \pm 1) g (I_1 - I_{1,I^{\pm}}). \tag{37}$$

However, since we want also to verify (32) we are immediately faced with a problem. In fact, with these choices in the expression for $v^{\pm} - w^{\pm}$ only one term, i.e., term $c^2_{i+1/2} = g[(A_i + A_{i+1})/(B_i + B_{i+1})]$, which is derived from $|\lambda^{(p)}_{i+1/2}|$ in (34) is evaluated at $(i + 1/2)$th cell boundary, while all the other values move over the entire stencil of points. Therefore, it will be impossible to obtain (32). However, we see that a similar term – term $(A + A_{I^{\pm}})/(B + B_{I^{\pm}})$ appears in (36), which comes from $\mathscr{V}$ (10) when included in (34). Therefore, if instead of $\mathscr{V}$ in (34) we use

$$\begin{pmatrix} 0 \\ g\left(I''_1 - I'_1\right) - c^2_{i+1/2}\left(A'' - A'\right) \end{pmatrix} \tag{38}$$

we easily see that (32) is verified. According with the presented algorithm we can conclude that with that modification the new balanced WENO-LLF schemes for (1) are constructed.

2.2. The Roe with entropy fix formulation

Now we can concentrate on the Roe with entropy fix (RF) formulation. Entropy fix in the RF formulation means that if eigenvalue changes sign at some cell boundary, then instead of the Roe formulation there the LLF formulation should be applied. Since we resolved the problem of the extension of the LLF formulation in Section 2.1, in this section we just have to deal with the pure Roe formulation. Also, since the reasoning is very similar to the one in that section, here we give just the key expressions and results.

For the construction of the new RF formulation, we compare the original Roe formulation with the simple upwind scheme and numerically approximate the flux and the source term using relations

$$f^{(p)}_{i+1/2} = f^{(p)}_{i+1/2,\text{upwind}} + \mathscr{P}^{(p)}_{i+1/2,+} + \mathscr{P}^{(p)}_{i+1/2,-}, \tag{39}$$

$$g^{(p)}_{i+1/2,L} = g^{(p)}_{i+1/2,L,\text{upwind}} + \frac{1}{\Delta x}\mathscr{Q}^{(p)}_{i+1/2,+} + \frac{1}{\Delta x}\mathscr{Q}^{(p)}_{i+1/2,-}, \tag{40}$$

$$g^{(p)}_{i+1/2,R} = g^{(p)}_{i+1/2,R,\text{upwind}} - \frac{1}{\Delta x}\mathscr{Q}^{(p)}_{i+1/2,+} - \frac{1}{\Delta x}\mathscr{Q}^{(p)}_{i+1/2,-}. \tag{41}$$

Here, the upwind parts are given with

$$f^{(p)}_{i+1/2,\text{upwind}} = \left(\frac{1 + \text{sign}\left(\lambda^{(p)}_{i+1/2}\right)}{2}\mathbf{f}_i + \frac{1 - \text{sign}\left(\lambda^{(p)}_{i+1/2}\right)}{2}\mathbf{f}_{i+1}\right) \cdot \mathbf{l}^{(p)}_{i+1/2}, \tag{42}$$

$$g^{(p)}_{i+1/2,L,\text{upwind}} = \frac{1 - \text{sign}\left(\lambda^{(p)}_{i+1/2}\right)}{2}\mathbf{g}_{i+1/2} \cdot \mathbf{l}^{(p)}_{i+1/2}, \tag{43}$$

$$g^{(p)}_{i+1/2,R,\text{upwind}} = \frac{1 + \text{sign}\left(\lambda^{(p)}_{i+1/2}\right)}{2}\mathbf{g}_{i+1/2} \cdot \mathbf{l}^{(p)}_{i+1/2}. \tag{44}$$

Terms $\mathscr{P}^{(p)}_{i+1/2,\pm}$ and $\mathscr{Q}^{(p)}_{i+1/2,\pm}$ are again high-order WENO reconstructions. Therefore, we compute them in the same way as described in Section 2.1, however now, following [29], using functions:

$$v^{\pm} = \frac{1 \pm \text{sign}\left(\lambda^{(p)}_{i+1/2}\right)}{2}\left(\mathbf{f} - \mathbf{f}_{I^{\pm}}\right) \cdot \mathbf{l}^{(p)}_{i+1/2}, \tag{45}$$

$$w^{\pm} = \frac{1 \pm \operatorname{sign}\left(\lambda^{(p)}_{i+1/2}\right)}{2} \mathscr{G}(\mathbf{u}_{I^{\pm}}, \mathbf{u}, x_{I^{\pm}}, x) \cdot \mathbf{l}^{(p)}_{i+1/2}. \tag{46}$$

Here, $I^{+} = i$ and $I^{-} = i + 1$, just as before. In particular, for (1) under quiescent flow conditions (16) these function become

$$v^{\pm} = \frac{1}{2c_{i+1/2}}((-1)^{p} \pm 1) g(I_1 - I_{1,I^{\pm}}), \tag{47}$$

$$w^{\pm} = \frac{1}{2c_{i+1/2}}((-1)^{p} \pm 1) g(I_1 - I_{1,I^{\pm}}). \tag{48}$$

Therefore, now no factor evaluated at $(i + 1/2)$th cell boundary appears in the expressions, (32) is immediately satisfied and there is no need for further modification of the proposed algorithm.

3. Extension of WENO schemes to one-dimensional elastic wave equations

The one-dimensional elastic wave equations [1] are balance laws of type (2) with

$$\mathbf{u} = \begin{pmatrix} \rho\epsilon \\ \rho u \end{pmatrix}, \quad \mathbf{f} = \begin{pmatrix} -\rho u \\ -\sigma \end{pmatrix}, \quad \mathbf{g} = \begin{pmatrix} -u\frac{\mathrm{d}\rho}{\mathrm{d}x} \\ 0 \end{pmatrix}. \tag{49}$$

Here, $\rho = \rho(x)$ is the media density, $\epsilon = \epsilon(x, t)$ is the strain, $u = u(x, t)$ is the velocity, and σ is the stress defined with a stress–strain relation $\sigma = \sigma(\epsilon, x)$. In the case of the linear acoustics the stress–strain relation is $\sigma(\epsilon, x) = K\epsilon$, where $K = K(x)$ is the bulk modulus of compressibility. If the stress–strain relation is nonlinear, for example if it is given with

$$\sigma(\epsilon, x) = \rho\epsilon + 0.3(\rho\epsilon)^2, \tag{50}$$

it is the nonlinear acoustics case.

Since the process of extending WENO schemes to the elastic wave equations is very similar to the one we presented in Section 2 for the open channel flow case, we present here only what is different. Also, we want to emphasize that our goal now is to obtain consistency of the schemes with all the steady-state solutions, and these are characterized with $\sigma = \text{const.}$ and $u = \text{const.}$

In the construction of the schemes, first we find numerical approximations for $\mathbf{v}\,\mathrm{d}x$ and for $\mathbf{g}\,\mathrm{d}x$,

$$\mathscr{V} = \begin{pmatrix} 0 \\ -(\sigma'' - \sigma') - \beta(\rho''\epsilon'' - \rho'\epsilon') \end{pmatrix}, \tag{51}$$

$$\mathscr{G} = \begin{pmatrix} -\frac{u' + u''}{2}(\rho'' - \rho') \\ 0 \end{pmatrix}. \tag{52}$$

Here,

$$\beta = \frac{K' + K''}{\rho' + \rho''}, \tag{53}$$

in the case of linear acoustics, or

$$\beta = 1 + 0.6\frac{\epsilon' + \epsilon''}{2}\frac{\rho' + \rho''}{2}, \tag{54}$$

in the case of nonlinear acoustics with stress–strain relation (50).

Then, we compute the extended Roe average (6)

$$c_{i+1/2} = \frac{K_i + K_{i+1}}{\rho_i + \rho_{i+1}}, \tag{55}$$

in the linear acoustics case, or

$$c_{i+1/2} = 1 + 0.6\frac{\epsilon_i + \epsilon_{i+1}}{2}\frac{\rho_i + \rho_{i+1}}{2}, \tag{56}$$

in the case of nonlinear acoustics with stress–strain relation (50). Here, $c = \sqrt{(1/\rho)(\partial\sigma/\partial\epsilon)|_{x=\text{const.}}}$ is the wave speed.

Furthermore, in the WENO-LLF formulation we again use (17)–(19), (22)–(24), (29) and (30). Morover, if we try with (34) and (35), under steady-state conditions we again have the problem with factor $c^2_{i+1/2}$ that prevents (32) to be true, just as it was the case in the previous section. In fact, this problem can be solved in a similar way as in the open channel flow equations case. We can find a term similar to $c^2_{i+1/2}$ in $\mathscr{V}$ (51) – the term β and then put

$$\begin{pmatrix} 0 \\ -(\sigma'' - \sigma') - c^2_{i+1/2}(\rho''\epsilon'' - \rho'\epsilon') \end{pmatrix}, \tag{57}$$

instead of $\mathscr{V}$ in (34). With that choice, the modification to the WENO-LLF schemes are completed.

In a similar way, we can see that (29), (30) and (39)–(46) as we suggested in [29], with no further modifications present the valid new WENO-RF algorithm.

4. Generalized algorithm

In [29] we proposed an extension of the finite difference WENO schemes, which were originally developed for hyperbolic systems of conservation laws [2,15,16,19,25–27] to new finite difference WENO schemes for hyperbolic systems of balance laws with a geometrical source term. In Sections 2 and 3 we go one step further and find appropriate extensions of the same schemes to two hyperbolic systems of balance laws: open channel flow equations (1) and elastic wave equations (49). Both examined balanced laws have the geometrical source term and an additional difficulty – spatially variable flux. In fact, the ideas proposed in [29] and in Sections 2 and 3 can be expressed as one generalized algorithm as follows.

In any extended finite difference WENO scheme we use expressions (4) and (5). Then, for the LLF formulation we use (17)–(19), (22)–(24), (29), and (30). Furthermore, since for $v^{\pm}$ and $w^{\pm}$ we cannot use (34) and (35) we proceed as follows. First we establish what is the value of the factor $|\lambda^{(p)}_{i+1/2}|$ for the particular steady-state solution subset. Obviously, this value is an average expression between states $\mathbf{u}_i$ and $\mathbf{u}_{i+1}$. Then we can easily generalize that expression to the average between any two states $\mathbf{u}'$ and $\mathbf{u}''$ and try to find such a term in $\mathscr{V}$, as we did in the previous two sections, or in $\mathscr{G}$ as we did in [29]. That term, if found in $\mathscr{V}$ or $\mathscr{G}$ we denote as β or γ, respectively. Then we can split $\mathscr{V}$ and $\mathscr{G}$ so that the following relations are valid:

$$\mathscr{V}(\mathbf{u}', \mathbf{u}'', x', x'') = \mathscr{V}_1(\mathbf{u}', \mathbf{u}'', x', x'') + \beta(\mathbf{u}', \mathbf{u}'', x', x'')\mathscr{V}_2(\mathbf{u}', \mathbf{u}'', x', x''), \tag{58}$$

$$\mathscr{G}(\mathbf{u}', \mathbf{u}'', x', x'') = \mathscr{G}_1(\mathbf{u}', \mathbf{u}'', x', x'') = \gamma(\mathbf{u}', \mathbf{u}'', x', x'')\mathscr{G}_2(\mathbf{u}', \mathbf{u}'', x', x''). \tag{59}$$

These relations work well for all the hyperbolic balance laws that we examined, so they are a good guideline in general. Furthermore, we take $\beta_{i+1/2} = \beta(\mathbf{u}_i, \mathbf{u}_{i+1}, x_i, x_{i+1})$ and $\gamma_{i+1/2} = \gamma(\mathbf{u}_i, \mathbf{u}_{i+1}, x_i, x_{i+1})$, and then define the appropriate expression for functions $v^{\pm}$ and $w^{\pm}$ with

$$v^{\pm} = \frac{1}{2}\left((\mathbf{f} - \mathbf{f}_{I^{\pm}}) \pm \left|\lambda^{(p)}_{i+1/2}\right|(\mathbf{u} - \mathbf{u}_{I^{\pm}}) \pm \operatorname{sign}\left(\lambda^{(p)}_{i+1/2}\right)\left(\mathscr{V}_1(\mathbf{u}_{I^{\pm}}, \mathbf{u}, x_{I^{\pm}}, x) + \beta_{i+1/2}\mathscr{V}_2(\mathbf{u}_{I^{\pm}}, \mathbf{u}, x_{I^{\pm}}, x)\right)\right) \cdot \mathbf{l}^{(p)}_{i+1/2}, \tag{60}$$

$$w^{\pm} = \frac{1}{2}\left(\mathscr{G}_1(\mathbf{u}_{I^{\pm}}, \mathbf{u}, x_{I^{\pm}}, x) \pm \operatorname{sign}\left(\lambda^{(p)}_{i+1/2}\right)\gamma_{i+1/2}\mathscr{G}_2(\mathbf{u}_{I^{\pm}}, \mathbf{u}, x_{I^{\pm}}, x)\right) \cdot \mathbf{l}^{(p)}_{i+1/2}. \tag{61}$$

First of all, these expressions are again acceptable numerical approximation for $\mathbf{f}$ and $\mathbf{g}\,\mathrm{d}x$. On the other hand, if we combine them into $v^{\pm} - w^{\pm}$, we can separate terms that contain factors evaluated at $(i + 1/2)$th cell boundary from the other terms. We can even generalize a little bit and define two new functions

$$\phi_1(\mathbf{u}', \mathbf{u}'', x', x'') = (\mathbf{f}(\mathbf{u}'', x'') - \mathbf{f}(\mathbf{u}', x') - \mathscr{G}_1(\mathbf{u}', \mathbf{u}'', x', x'')) \cdot \mathbf{l}^{(p)}_{i+1/2}, \tag{62}$$

$$\begin{aligned}\phi_2(\mathbf{u}', \mathbf{u}'', x', x'') = \Big(&\left|\lambda^{(p)}_{i+1/2}\right|(\mathbf{u}'' - \mathbf{u}') + \operatorname{sign}\left(\lambda^{(p)}_{i+1/2}\right)\left(\mathscr{V}_1(\mathbf{u}', \mathbf{u}'', x', x'') + \beta_{i+1/2}\mathscr{V}_2(\mathbf{u}', \mathbf{u}'', x', x'')\right) \\ &- \operatorname{sign}\left(\lambda^{(p)}_{i+1/2}\right)\gamma_{i+1/2}\mathscr{G}_2(\mathbf{u}', \mathbf{u}'', x', x'')\Big) \cdot \mathbf{l}^{(p)}_{i+1/2}.\end{aligned} \tag{63}$$

Obviously $v^{\pm} - w^{\pm} = \phi_1(\mathbf{u}_{I^{\pm}}, \mathbf{u}, x_{I^{\pm}}, x) + \phi_2(\mathbf{u}_{I^{\pm}}, \mathbf{u}, x_{I^{\pm}}, x)$. Therefore, if for the chosen steady-state solutions we can prove

$$\phi_1(\mathbf{u}', \mathbf{u}'', x', x'') = 0 \quad \text{and} \quad \phi_2(\mathbf{u}', \mathbf{u}'', x', x'') = 0, \tag{64}$$

then (32) is also true, i.e., the new scheme is consistent with that subset of steady-state solutions. Conditions in (64) are not artificial. They can be verified in all the hyperbolic balance laws we examined. Even more, we can easily see that if these conditions are satisfied the appropriate Q-scheme will have the exact conservation property too. With this we concluded the generalized WENO-LLF algorithm.

In the RF formulation we use (29), (30), and (39)–(44). Furthermore, expressions (45) and (46), that we suggested in [29] work well. Therefore, no further modifications are needed. In particular, only one condition for the exact conservation property must be satisfied and it is exactly the first condition in (64). Thus, we see that with the correct construction of the balanced LLF algorithm for any particular hyperbolic system of balance laws, the construction and balancing of the RF formulation is automatically solved. In fact, comparison with the Q-scheme part terms or upwind scheme part terms shows even more – the correct construction of the balanced LLF algorithm also solves appropriate well-balanced application of these schemes for any balance law system in consideration.

5. Numerical results

In this section we present results for one convergence test on a linear acoustics problem, four open channel flow test problems, and four elastic wave test problems. If not stated otherwise, in all computations we use three-step Runge–Kutta time integration and we take [19]

$$\Delta t \propto (\Delta x)^{R/3}. \tag{65}$$

Here R is the theoretical order of the used ENO or WENO reconstruction. More precisely, if the function under ENO or WENO reconstruction is smooth enough, then the resulting reconstruction is of Rth order of accuracy, where $R = r + 1$ or $R = 2r + 1$, respectively. Relation (65) guarantees that accuracy in time, which is $O(\Delta t^3)$ since we always use three-step, i.e., third-order Runge–Kutta method, is the same as the accuracy in space, which is of course $O(\Delta x^R)$. Also, if not stated otherwise, we use CFL coefficient $c_{\mathrm{cfl}} = 0.8$.

5.1. A convergence test

First of all, we present experimentally obtained orders of accuracy for the new schemes. In order to do this we use a Cauchy problem in linear acoustics. We obtained this problem by modifying a test problem from [1]. Since ENO or WENO reconstruction is of high order only for smooth functions, we use smooth media properties and smooth initial data. In particular, the initial state is given with

$$\sigma(\epsilon(x,0)x) = -1 - 1.5e^{-(8x)^2}, \quad u(x,0) = 0, \tag{66}$$

while the sound speed and impendance $Z = \rho c$ of the media are given with

$$c(x) = 1 - 0.5\sin(\pi x), \quad Z(x) = 1. \tag{67}$$

Since we do not know the exact solution for this problem, as a substitution we use numerical solution obtained with pointwise WENO-RF, $r = 5$ on the grid with 1280 points after $t = 0.001$ s from the beginning of the propagation of the pulse in pressure. Then we compute L^∞ and L^1 errors and orders for solutions obtained on much coarser grids of 10, 20, etc. points over the comparison interval $[-1, 1]$. Table 1 shows that there is almost no difference in computed orders of accuracy between pointwise and balanced versions of schemes. In particular, Table 1 contains results for $r = 5$ case, but other values $r = 1$, 2, 3, and 4 for which we performed computations show the same trend. Also, in Tables 1–3 we can see that the experi-

Table 1
The convergence test results for RF, $r = 5$ schemes, Section 5.1

Method	No. of cells	10	20	40	80
Bal. ENO, $R = 6$	L^∞ error	3.9867×10^{-4}	6.2253×10^{-5}	6.6501×10^{-6}	2.5451×10^{-7}
	L^∞ order	–	2.68	3.23	4.71
Point. ENO, $R = 6$	L^∞ error	3.5749×10^{-4}	6.2253×10^{-5}	6.6541×10^{-6}	2.5483×10^{-7}
	L^∞ order	–	2.52	3.23	4.71
Bal. WENO, $R = 11$	L^∞ error	3.8744×10^{-4}	9.2013×10^{-5}	2.5937×10^{-6}	7.4077×10^{-9}
	L^∞ order	–	2.07	5.15	8.45
Point. WENO, $R = 11$	L^∞ error	3.8744×10^{-4}	9.2010×10^{-5}	2.5920×10^{-6}	6.9258×10^{-9}
	L^∞ order	–	2.07	5.15	8.55

Table 2
The convergence test results for balanced ENO-RF schemes, Section 5.1

Method	No. of cells	10	20	40	80	160
$r = 1$, $R = 2$	L^∞ error	3.3901×10^{-4}	1.5969×10^{-4}	1.6126×10^{-4}	1.0601×10^{-4}	5.7251×10^{-5}
	L^∞ order	–	1.09	−0.01	0.61	0.89
$r = 2$, $R = 3$	L^∞ error	4.9500×10^{-4}	1.4359×10^{-4}	5.3350×10^{-5}	1.2019×10^{-5}	1.6934×10^{-6}
	L^∞ order	–	1.79	1.43	2.15	2.83
$r = 3$, $R = 4$	L^∞ error	1.5392×10^{-4}	1.0192×10^{-4}	2.6560×10^{-5}	3.7277×10^{-6}	5.5567×10^{-7}
	L^∞ order	–	0.59	1.94	2.83	2.75
$r = 4$, $R = 5$	L^∞ error	1.1740×10^{-4}	7.1203×10^{-5}	1.0487×10^{-5}	8.4816×10^{-7}	3.2901×10^{-8}
	L^∞ order	–	0.72	2.76	3.03	4.69

Table 3
The convergence test results for balanced WENO-RF schemes, Section 5.1

Method	No. of cells	10	20	40	80	160
$r = 1$, $R = 3$	L^∞ error	5.6548×10^{-4}	2.4381×10^{-4}	1.4108×10^{-4}	7.5150×10^{-5}	3.7468×10^{-5}
	L^∞ order	–	1.21	0.79	0.91	1.00
$r = 2$, $R = 5$	L^∞ error	4.9500×10^{-4}	1.8093×10^{-4}	2.4973×10^{-5}	2.1678×10^{-6}	1.2825×10^{-7}
	L^∞ order	–	1.45	2.86	3.53	4.08
$r = 3$, $R = 7$	L^∞ error	4.4948×10^{-4}	1.1190×10^{-4}	1.1858×10^{-5}	5.8425×10^{-7}	1.2531×10^{-8}
	L^∞ order	–	2.01	3.24	4.34	5.54
$r = 4$, $R = 9$	L^∞ error	4.1693×10^{-4}	1.0525×10^{-4}	5.7218×10^{-6}	2.1076×10^{-8}	8.6470×10^{-11}
	L^∞ order	–	1.99	4.20	8.08	7.93

mentally obtained orders are smaller but very close to the theoretical orders R. In all the three tables we present L^∞ errors and orders. As expected, the computed L^1 orders are better – in average for 0.5 bigger then the L^∞ ones. Therefore, we can conclude that the proposed modification that lead to the balancing of the schemes, did not deteriorate convergence properties of the schemes.

5.2. The quiescent flow and a tidal wave propagation in a channel proposed by the Working Group on Dam Break Modeling

In this subsection we present results for two open channel flow tests, both for the same channel geometry, which was proposed by the Working Group on Dam Break Modeling [14]. The observed channel has rectangular cross-section, very variable bed level and width (Fig. 1), and Manning's friction factor $M = 0.03$. In the first test the initial condition is the quiescent flow with water level equal to $H = 15$ m. Since no perturbation is introduced the quiescent flow stays preserved. In the second test the initial condition is the quiescent flow with water level $H = 12$ m. Then from the upstream end a tidal wave propagates while at the downstream end there is a wall

$$h(0,t) = 16 + 4\sin\left(\frac{(t-10,800)\pi}{21,600}\right), \quad Q(1500,t) = 0. \tag{68}$$

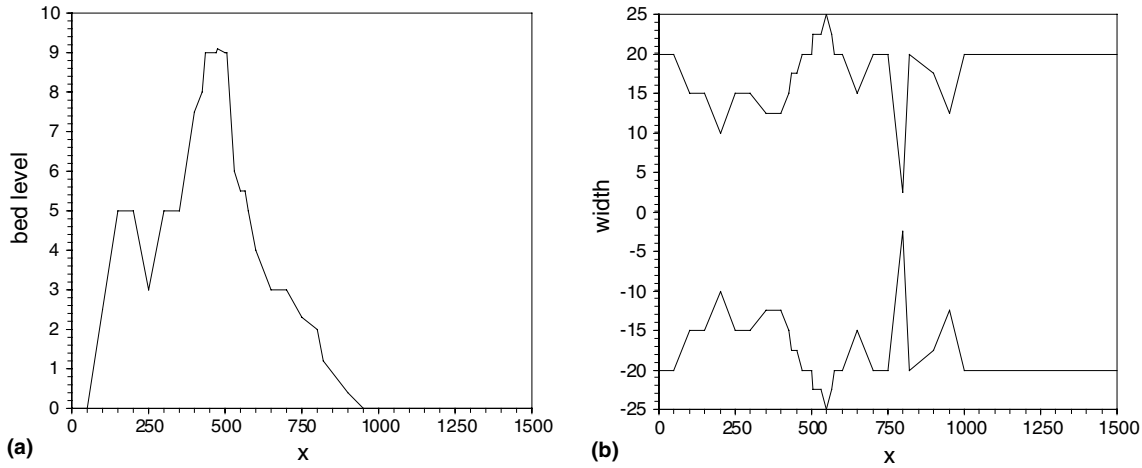

Fig. 1. (a) Channel bed level and (b) width as proposed by the Working Group on Dam Break Modeling, Section 5.2.

Table 4
L^∞ error for the quiescent flow test, Section 5.2

Method	H error		Q error	
	Bal. version	Point. version	Bal. version	Point. version
Q-scheme	9.948×10^{-14}	1.741×10^{0}	4.798×10^{-12}	2.480×10^{2}
Flux limited	9.948×10^{-14}	1.744×10^{0}	4.319×10^{-12}	2.188×10^{2}
ENO-LLF, $r = 1$	9.948×10^{-14}	1.551×10^{0}	8.397×10^{-12}	1.769×10^{2}
ENO-LLF, $r = 5$	9.948×10^{-14}	7.177×10^{-1}	6.673×10^{-12}	1.574×10^{2}
ENO-RF, $r = 1$	9.948×10^{-14}	9.630×10^{-1}	3.359×10^{-12}	1.423×10^{2}
ENO-RF, $r = 5$	9.948×10^{-14}	6.208×10^{-1}	8.197×10^{-12}	1.180×10^{2}
WENO-LLF, $r = 1$	9.948×10^{-14}	1.749×10^{0}	1.871×10^{-11}	1.510×10^{2}
WENO-LLF, $r = 5$	2.007×10^{-13}	1.893×10^{0}	5.716×10^{-11}	8.637×10^{1}
WENO-RF, $r = 1$	9.948×10^{-14}	9.085×10^{-1}	1.991×10^{-11}	1.330×10^{2}
WENO-RF, $r = 5$	2.007×10^{-13}	1.290×10^{0}	6.101×10^{-11}	6.683×10^{1}

In both tests, we perform all computations using space step $\Delta x = 2.5$ m. Results presented in Table 4 and Fig. 2 clearly demonstrate the superiority of the balanced version of the schemes when applied to quiescent flows and slowly varying nonstationary flows over highly irregular channel bed. In fact, in those cases the magnitude of the error in nonbalanced versions is of the same order as of the waves that propagate through the domain. Therefore the results obtained with these schemes have unacceptably large errors and only balanced versions can be used.

5.3. A stationary jump in a converging-diverging channel

In the open channel flow test contained in this section the channel is frictionless, rectangular, with horizontal bed and variable width [28]

$$B(x) = \begin{cases} 5 - 0.7065\left(1 + \cos\left(2\pi \frac{x-250}{300}\right)\right) & \text{if } |x - 250| \leqslant 150, \\ 5 & \text{otherwise.} \end{cases} \tag{69}$$

We test a steady-state flow with subcritical inflow of discharge $Q = 20$ m^3/s and a downstream weir, so that at the channel restriction a hydraulic jump occurs. We perform all computations using $\Delta x = 2.5$ m. Since channel geometry is smooth, performances of the pointwise and balanced version of the schemes, particularly on the water level (Fig. 3) are very similar and the advantages of the balanced ones are less obvious. However, if we make a closer look on the computed discharge (Fig. 3), we can see that pointwise version produces error in the zone of the restriction of the channel, however, of small magnitude since channel geometry is smooth. Both versions have a local difficulty with the discharge at the jump, similar to all other schemes applied to such problems. Furthermore, convergence history computed for the relative error in water depth and presented in Fig. 4 more obviously shows the advantage of the proposed balancing of WENO schemes. Also, this test is good for observing high resolution properties of the schemes since the solution has a discontinuity – the hydraulic jump.

5.4. Water wave propagation through a natural watercourse

In the last open channel flow test we consider one example of a natural watercourse. The observed section of the river is $L = 2400$ m long, with highly irregular geometry given with cross-sections (Fig. 5)

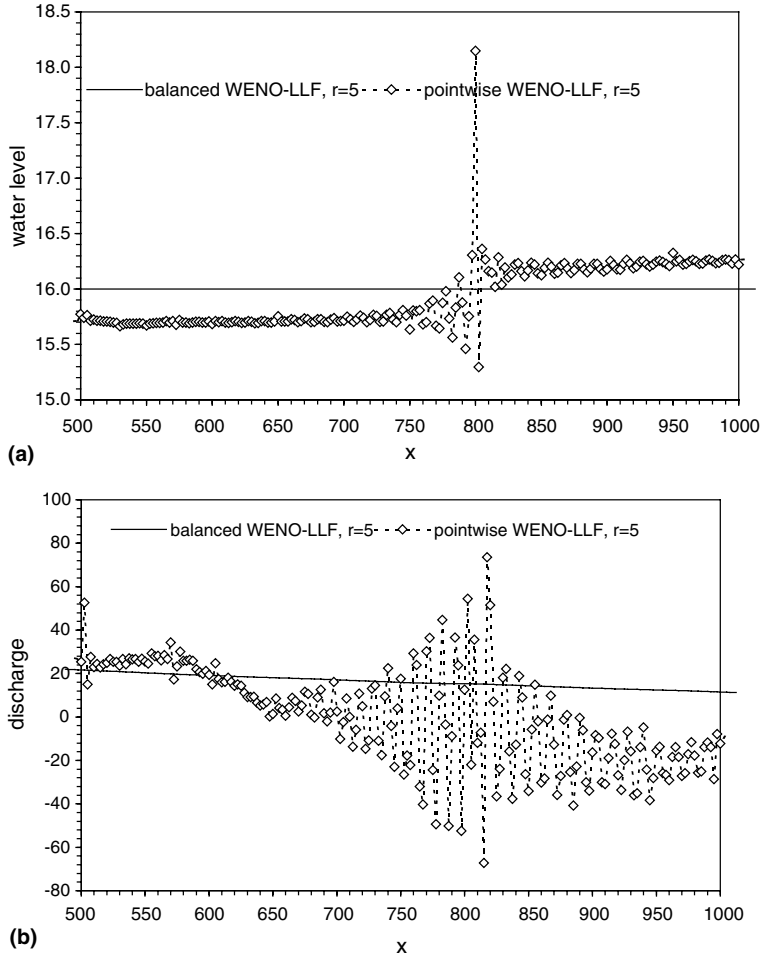

Fig. 2. (a) Water level and (b) discharge, after 3 h of tidal wave propagation, Section 5.2.

measured approximately every 50 m. The Manning's friction factor varies through the watercourse depending on the properties of the riverbed, with values between 0.03 and 0.05. The initial condition is quiescent flow with $H = 446$ m. Then after 120 s a sudden water wave propagates from the upstream boundary, i.e.

$$Q(0,t) = \begin{cases} 0 \text{ m}^3/\text{s} & \text{if } t \leqslant 120, \\ 50 \text{ m}^3/\text{s} & \text{otherwise}, \end{cases} \tag{70}$$

while at the downstream boundary the water level remains fixed. In all computations we use space step $\Delta x = 10$ m. Computational results in Figs. 6 and 7 show that differences between pointwise and balanced version are not significant in water level. However, some difficulties of the pointwise version can be observed in the water level over last 500 m of the river section where irregularity of the riverbed is higher and even a hydraulic jump occurs. On the other hand, the error in discharge when computed with pointwise

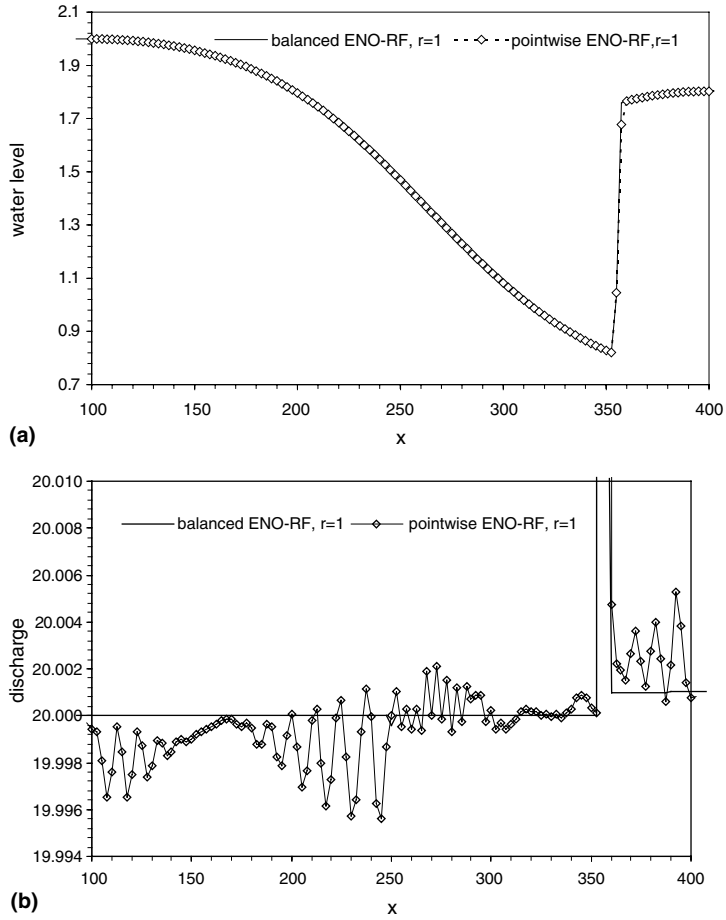

Fig. 3. (a) Water level and (b) discharge for the hydraulic jump test, Section 5.3.

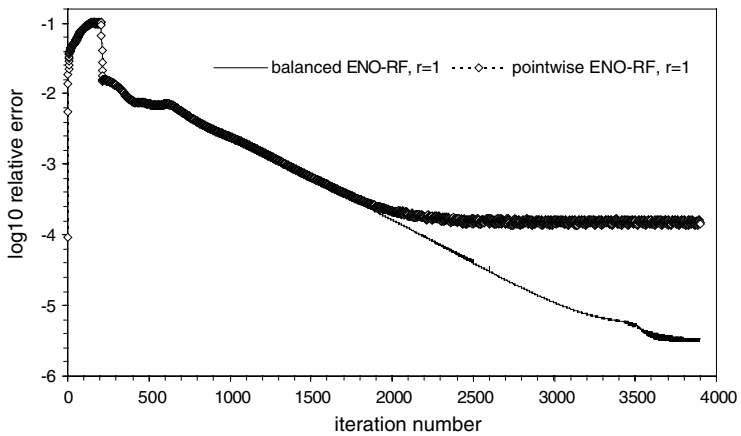

Fig. 4. Convergence history for the hydraulic jump test, Section 5.3.

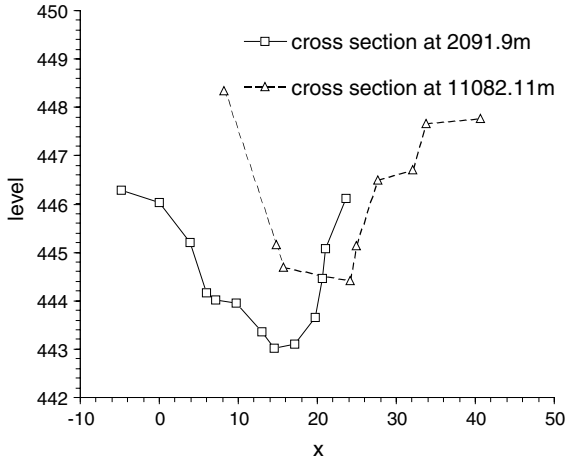

Fig. 5. Two cross-sections for one example of a natural watercourse, Section 5.4.

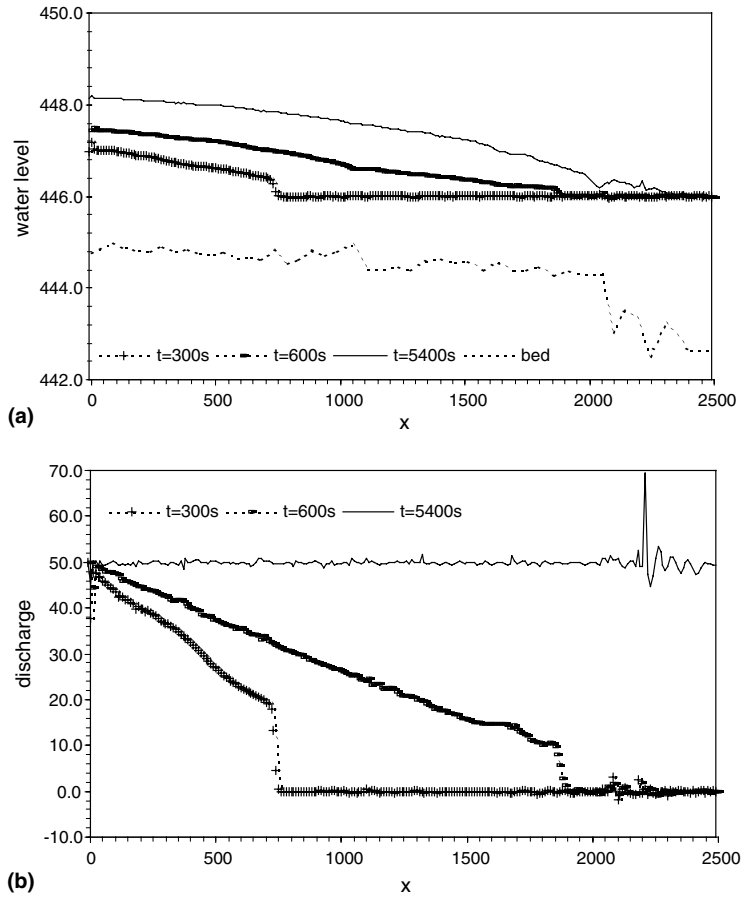

Fig. 6. (a) Water level and (b) discharge evolution computed with pointwise ENO-LLF, $r = 3$ scheme for the water wave propagation in a natural watercourse, Section 5.4.

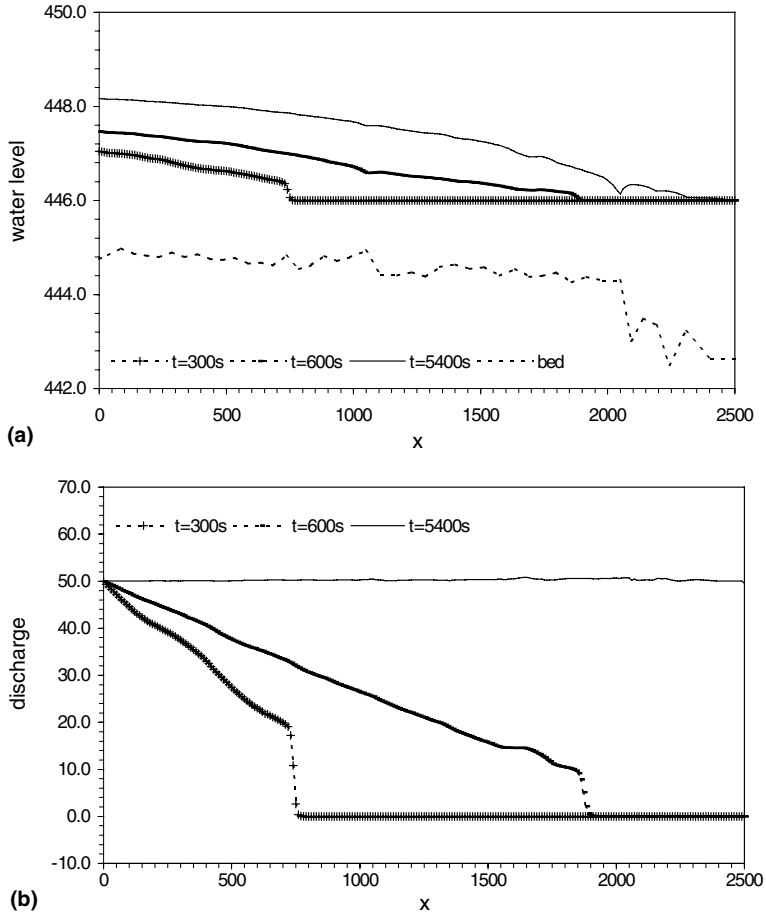

Fig. 7. (a) Water level and (b) discharge evolution computed with balanced ENO-LLF, $r = 3$ scheme for the water wave propagation in a natural watercourse, Section 5.4.

schemes is very visible and unacceptably large, while balanced versions give excellent results (Figs. 6 and 7). We would like to emphasize again that in this test problem as well as in the case of any other natural watercourse, the cross-sections of the channel are not rectangular. Therefore, such problems could not be computed if we did not discuss and solve the balancing for the general form of the open channel flow equations (Section 2).

5.5. Nonlinear elasticity in a rapidly varying medium

Both tests in this section are for the elastic wave model [1]. More precisely, a heterogeneous media with nonlinear stress–strain dependency (50) initially is in the state $u(x,0) = \epsilon(x,0) = 0$, and then a smooth pulse incomes from the left boundary

$$u(0,t) = \begin{cases} -\frac{1}{5}\left(1+\cos\left(\frac{\pi}{30}(t-30)\right)\right) & \text{if } t \leqslant 60, \\ 3 & \text{if } t > 60. \end{cases} \tag{71}$$

In the first test, the medium has a rapidly varying but continuous density $\rho(x) = 2 - \sin(\pi x)$, while in the second test the medium density has an additional difficulty – it is discontinuous

$$\rho(x) = \begin{cases} 1 & \text{if } 2j < x < 2j+1, \\ 3 & \text{if } 2j+1 < x < 2j+2. \end{cases} \tag{72}$$

In all computations we use space step $\Delta x = 0.1$. As expected, in the first, smooth case, the difference between pointwise and balanced versions is negligible. Therefore, we only present results obtained with balanced versions of different orders of accuracy (Fig. 8). These results show that contribution of the

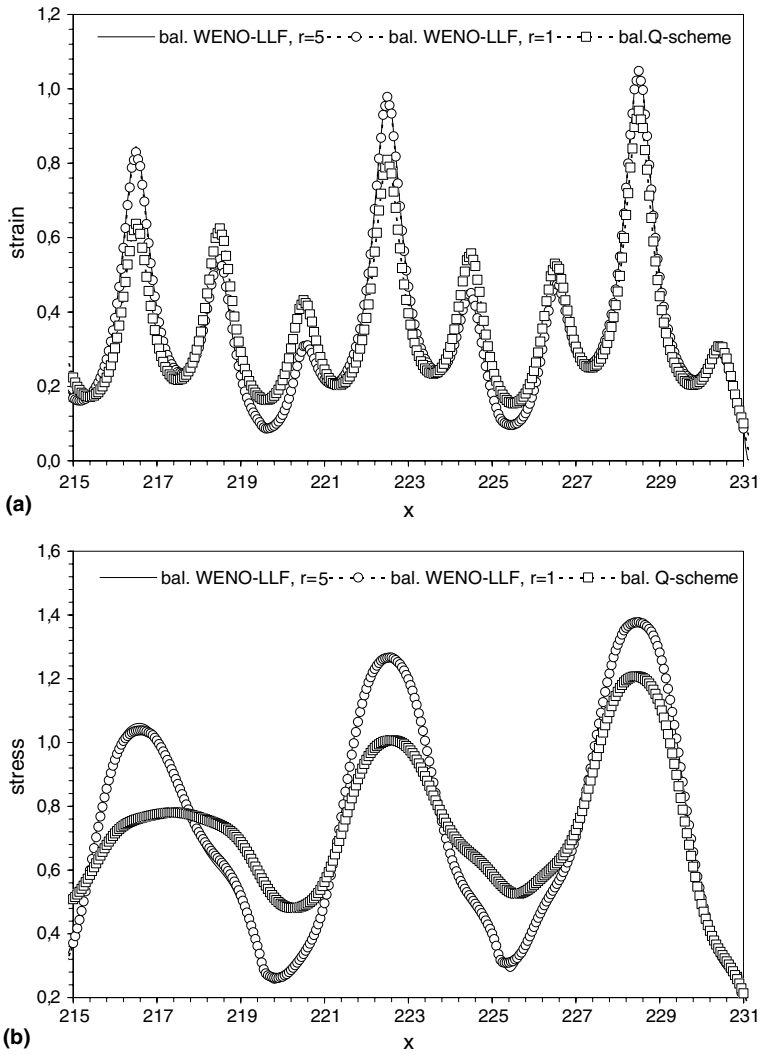

Fig. 8. (a) Strain and (b) stress at $t = 240$ s for the elastic wave propagation in a continuous media, Section 5.5.

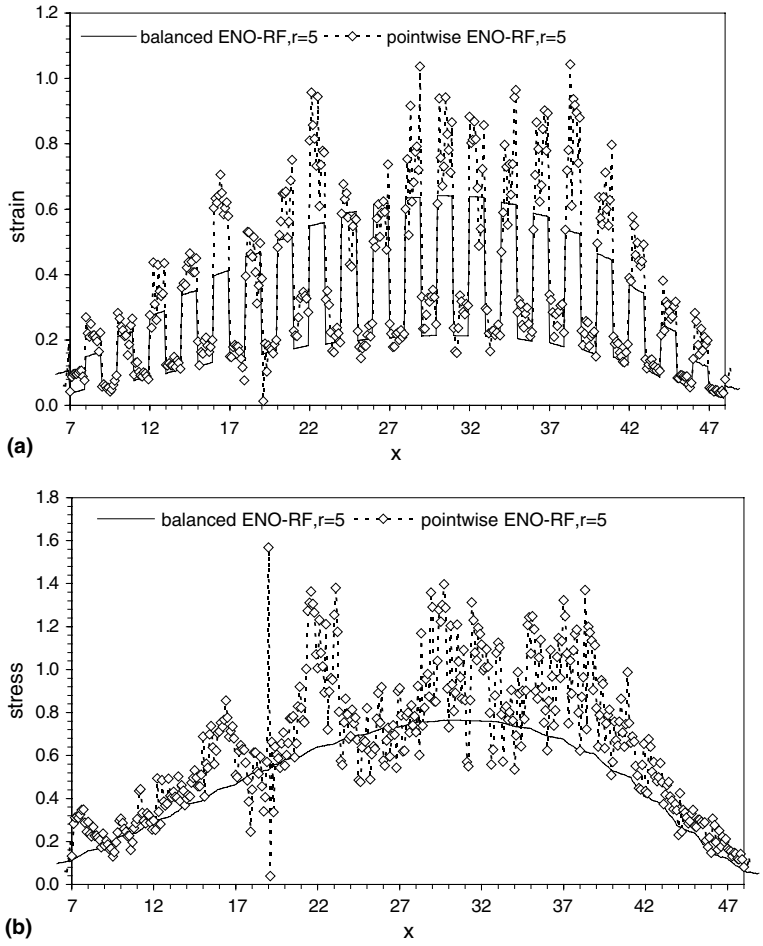

Fig. 9. (a) Strain and (b) stress at $t = 60$ s for the elastic wave propagation in a discontinuous media, Section 5.5.

increase of space order brings significant improvement in scheme resolution. In the second test with discontinuous media properties, error in pointwise version computations are very large. We present results obtained up to time $t = 60$ s (Fig. 9) since soon after that moment the error in pointwise scheme builds up so much that causes computational break down. As opposed to that, balanced scheme results present no difficulties. In particular, since the medium density is discontinuous, the high resolution property of the new schemes can be clearly observed in Fig. 9(a).

5.6. Linear acoustics

In this section we present results for two linear acoustics tests [1]. In both tests the initial conditions are given by $u(x) = 0$ and

$$\sigma(\epsilon(x,0)x) = \begin{cases} -\frac{7}{4} + \frac{3}{4}\cos(10\pi x - 4\pi) & \text{if } 0.4 < x < 0.6, \\ 1 & \text{otherwise.} \end{cases} \tag{73}$$

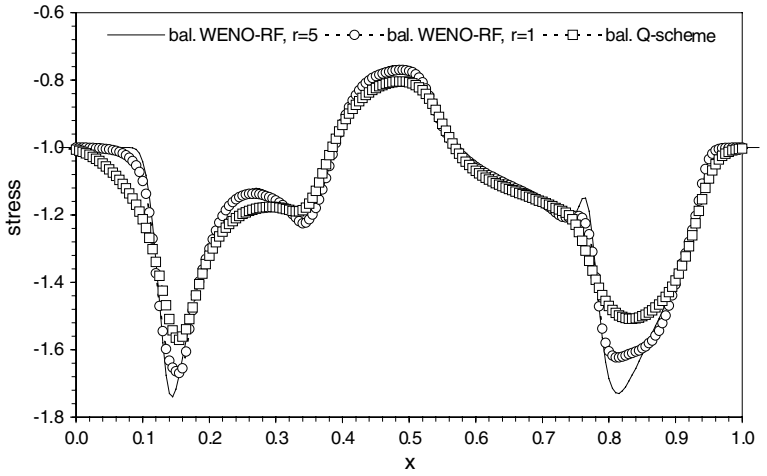

Fig. 10. Stress at $t = 0.40$ s for the first linear acoustics test, Section 5.6.

In the first test the properties of the media are given with

$$c(x) = 1 + 0.5\sin(10\pi x), \quad Z(x) = 1 + 0.25\cos(10\pi x), \tag{74}$$

and in the second test with

$$c(x) = \begin{cases} 0.6 & \text{if } 0.35 < x < 0.65, \\ 2 & \text{otherwise,} \end{cases} \quad Z(x) = \begin{cases} 6 & \text{if } 0.35 < x < 0.65, \\ 2 & \text{otherwise.} \end{cases} \tag{75}$$

We perform all computations using $\Delta x = 0.005$. Again, as expected, when the media has smooth properties (74) pointwise and balanced version results coincide while in the discontinuous case (75) the error in the pointwise version is extremely large (Fig. 11). Also, in both test cases increase in WENO reconstruction parameter r results in a significant increase in high resolution properties of the schemes (Figs. 10 and 11).

6. Concluding remarks

The new WENO schemes that we propose in this paper are aimed on solving hyperbolic systems of balance laws with spatially variable flux and geometrical source term. As we show here and in [29], when flux is not spatially variable the new algorithm reduces to the one designed for balance laws with geometrical source terms, which we presented in [29], and when in addition the balance laws are homogeneous, both algorithms reduce to the original WENO schemes.

We apply new schemes to the one-dimensional open channel flow equations and to the one-dimensional elastic wave equations. Naturally, application to the one-dimensional shallow water equations that we presented in [29] is valid for the new algorithm too. Since the new algorithm respects balancing between the flux gradient and the source term, we obtain schemes with exact conservation property, i.e., schemes consistent with appropriate steady-state solutions in both cases. We prove that property analytically and demonstrate it through several test problems. On the other hand, the same tests show that the original version of WENO schemes combined with only pointwise source term evaluation gives poor results when applied to nonsmooth data (channel geometry or media properties).

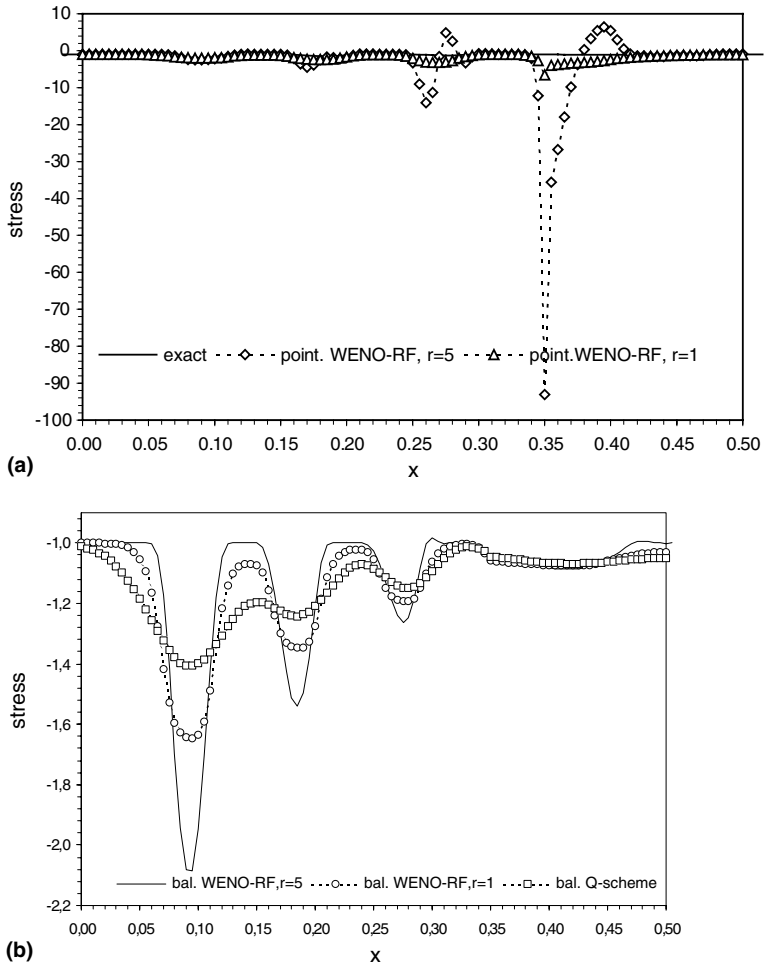

Fig. 11. (a) Pointwise vs. exact and (b) low vs. high-order schemes on the stress at $t = 0.50$ s for the second linear acoustics test, Section 5.6.

The results of a convergence test on a Cauchy problem for linear acoustic equations, lead us to the conclusion that modifications which we introduced into WENO schemes do not deteriorate order of accuracy when compared to original WENO schemes combined with pointwise source term evaluation. Therefore, the new schemes are high order, high resolution and shock capturing as much as the original WENO schemes are.

References

[1] D.S. Bale, R.J. LeVeque, S. Mitran, J.A. Rossmanith, A wave propagation method for conservation laws and balance laws with spatially varying flux functions (2001), preprint.
[2] D.S. Balsara, C.W. Shu, Monotonicity preserving weighted essentially nonoscillatory schemes with increasingly high order of accuracy, J. Comput. Phys. 160 (2000), doi:10.1006/jcph.2000.6443.
[3] A. Bermùdez, A. Dervieux, J.A. Désideéri, M.E. Vázquez, Upwind schemes for the two-dimensional shallow water equations with variable depth using unstructured meshes, Comput. Methods Appl. Mech. Eng. 155 (1998) 49.

[4] A. Bermùdez, M.E. Vázquez, Upwind methods for hyperbolic conservation laws with source terms, Comput. Fluids 23 (8) (1994) 1049.
[5] M.O. Bristeau, B. Perthame, Transport of pollutant in shallow water using kinetic schemes, in: ESAIM-Proceedings, vol. 10 – CEMRACS, 1999, p. 9.
[6] J. Burguete, P. García–Navarro, Efficient construction of high-resolution TVD conservative schemes for equations with source terms: application to shallow water flows, Int. J. Numer. Meth. Fluids 37 (2001), doi: 10.1002/fld.175.
[7] A. Chinnaya, A.-Y. LeRoux, A new general Riemann solver for the shallow water equations, with friction topography. Available from: <www.math.ntnu.no/conservation/1999/021.html>.
[8] N. Crnjaric-Zic, S. Vukovic, L. Sopta, Extension of ENO and WENO schemes to one-dimensional bed-load sediment transport equations, Comput. Fluids 33 (1) (2003) 31.
[9] P. García–Navarro, F. Alcrudo, J.M. Saviroón, 1-D open-channel flow simulation using TVD-McCormack scheme, J. Hydraulic Eng. 118 (1992) 1359.
[10] P. García-Navarro, M.E. Vázquez-Cendón, On numerical treatment of the source terms in the shallow water equations, Comput. Fluids 29 (2000) 951.
[11] J.M. Greenberg, A.-Y. LeRoux, A well-balanced scheme for the numerical processing of source terms in hyperbolic equations, SIAM J. Numer. Anal. 33 (1996) 1.
[12] L. Gosse, A well-balanced flux-vector splitting scheme designed for hyperbolic systems of conservation laws with source terms, Comput. Math. Appl. 39 (2000) 135.
[13] L. Gosse, A well-balanced scheme using non-conservative products designed for hyperbolic systems of conservation laws with source terms, Math. Models Methods Appl. Sci. 11 (2001) 339.
[14] P. Goutal, F. Maurel, Proceedings of the 2nd Workshop on Dam Break Wave Simulation, Technical Report IIE-13/97/016A, Electricité de France, Département Laboratoire National d'Hydraulique, Groupe Hydraulique Fluviale, 1997.
[15] A. Harten, S. Osher, Uniformly high-order accurate non-oscillatory schemes, I, SIAM J. Numer. Anal. 24 (1987) 279.
[16] A. Harten, B. Engquist, S. Osher, S.R. Chakravarthy, Uniformly high-order accurate non-oscillatory schemes, III, J. Comput. Phys. 71 (1987) 231.
[17] M.E. Hubbard, P. García–Navarro, Flux difference splitting and the balancing of source terms and flux gradients, J. Comput. Phys. 165 (2000), doi: 10.1006/jcph.2000.6603.
[18] P. Jenny, B. Müller, Rankine–Hugoniot–Riemann solver considering source terms and multidimensional effects, J. Comput. Phys. 145 (1998) 575.
[19] G. Jiang, C.W. Shu, Efficient implementation of weighted ENO schemes, J. Comput. Phys. 126 (1996) 202.
[20] S. Jin, A steady-state capturing method for hyperbolic systems with geometrical source terms, Math. Model. Numer. Anal. 35 (2001) 631.
[21] R.J. LeVeque, Balancing source terms and flux gradients in high-resolution Godunov methods: the quasi-steady wave-propagation algorithm, J. Comput. Phys. 146 (1998) 346.
[22] X.-D. Liu, S. Osher, T. Chan, Weighted essentially non-oscillatory schemes, J. Comput. Phys. 115 (1994) 200.
[23] B. Perthame, C. Simeoni, A kinetic scheme for the Saint-Venant system with a source term, CALCOLO 38 (4) (2001) 201.
[24] P.L. Roe, Upwinded difference schemes for hyperbolic conservation laws with source terms, in: A.S. Carasso, P.A. Raviart, J.P. Serre (Eds.), Proceedings of the Conference on Hyperbolic Problems, Springer, Berlin, 1986, p. 41.
[25] C.W. Shu, S. Osher, Efficient implementation of essentially non-oscillatory shock-capturing schemes, J. Comput. Phys. 77 (1988) 439.
[26] C.W. Shu, S. Osher, Efficient implementation of essentially non-oscillatory shock-capturing schemes, II, J. Comput. Phys. 83 (1989) 32.
[27] C.W. Shu, Essentially non-oscillatory and weighted essentially non-oscillatory shock-capturing schemes for hyperbolic conservation laws, in: B. Cockburn, C. Johnson, C.W. Shu, E. Tadmor (Eds.), Advanced Numerical Approximation of Nonlinear Hyperbolic Equations, Lecture Notes in Mathematics, vol. 1697, Springer, Berlin, 1988, p. 325.
[28] M.E. Vázquez-Cendón, Improved treatment of source terms in upwind schemes for the shallow water equations in channels with irregular geometry, J. Comput. Phys. 148 (1999) 497.
[29] S. Vukovic, L. Sopta, ENO and WENO schemes with the exact conservation property for one-dimensional shallow water equations, J. Comput. Phys. 179 (2002) 593, doi: 10.1006/jcph.2002.7076.
[30] S. Vukovic, L. Sopta, Upwind schemes with exact conservation property for one-dimensional open channel flow equations, SIAM J. Scient. Comput. 24 (5) (2003) 1630.
[31] J.G. Zhou, D.M. Causon, C.G. Mingham, D.M. Ingram, The surface gradient method for the treatment of source terms in the shallow water equations, J. Comput. Phys. 168 (2001) 1, doi:10.1006/jcph/2000.6670.